PRODUCTION OF $Q^2\overline{Q}^2$ STATES*

BING AN LI**

Stanford Linear Accelerator Center
Stanford University, Stanford, CA 94309

ABSTRACT

In this talk, the productions of $Q^2\overline{Q}^2$ states in two-photon collision and J/ψ radiative decays are discussed.

1. Introduction. The spectrum of low-lying hadrons is richer in the mass range of 1–2 GeV. Besides the $Q^2\overline{Q}^2$ mesons, some new types of hadrons, like glueballs and hybrids, are predicted theoretically. It is learned from the MIT bag model[1] that among the $Q^2\overline{Q}^2$ mesons, some decay to vector meson pairs dominantly and their masses are just about the threshold of corresponding vector meson pairs. These $Q^2\overline{Q}^2$ mesons might be observed as mass bumps.

The wave functions of some $Q^2\overline{Q}^2$ states can be projected to a color-singlet/color-singlet meson pair and a color-octet/color-octet meson pair. The recoupling coefficients for 0^+ $Q^2\overline{Q}^2$ states are the following (Jaffe's notations are used):

* Work supported by U.S. Department of Energy contracts DE–AC03–76SF00515; NSP–RII–8610671; and the Research Committee of the University of Kentucky.

** On leave from the Department of Physics and Astronomy, University of Kentucky; permanent address: Graduate School, University of Science and Technology of China.

	PP	VV	$\underline{P} \cdot \underline{P}$	$\underline{V} \cdot \underline{V}$
9	0.743	−0.041	−0.169	0.646
36	0.644	0.177	0.407	0.623
9*	−0.177	0.644	0.623	0.407
36*	0.041	0.743	−0.643	−0.169

For 2^+ $Q^2\overline{Q}^2$ states, the recoupling coeficients are:

	VV	$\underline{V} \cdot \underline{V}$
9	$\sqrt{\frac{2}{3}}$	$-\frac{1}{\sqrt{3}}$
36	$\frac{1}{\sqrt{3}}$	$\sqrt{\frac{2}{3}}$

According to the MIT bag model, the relative angular momenta of these states are s-waves. From these coefficients, the 0^+ (9^+, 36^+) and 2^+ (9, 36) states decay to vector pairs dominantly through the fall-apart mechanism.

On the other hand, according to the VDM, these states can be produced in two-photon collisions (Fig. 1). Also, due to the fact that there are color-octet-vector/color-octet-vector ($\underline{V} \cdot \underline{V}$) components in these states, we expect these states can be produced via two hard gluon channels in the mechanism, which is analogous to VDM^2 (Fig. 2). It is known from perturbative QCD that the J/ψ radiative decay provides such a two-gluon channel; therefore, the productions of these $Q^2\overline{Q}^2$ states are predicted in J/ψ radiative decays.

2. $Q^2\overline{Q}^2$ Production in $\gamma\gamma$ Collision. Under the mechanism of VDM, the $Q^2\overline{Q}^2$ states which decay to two-vector mesons dominantly can be produced in two-photon collisions (Fig. 1). Therefore, we can search for these $Q^2\overline{Q}^2$ states in the processes $\gamma\gamma \to VV'$.

$\gamma\gamma \to \rho^0\rho^0$ and $\rho^+\rho^-$. The experimental data[3] show large *enhancement* around the threshold of $\rho\rho$ in the cross section of $\gamma\gamma \to \rho^0\rho^0$. Other observations,[4] however, reveal large *suppression* in $\gamma\gamma \to \rho^+\rho^-$ around the $\rho\rho$ threshold. There are many attempts to explain these results; however, only the scheme of $Q^2\overline{Q}^2$ (Refs. 5, 6) survives. In the scheme of $Q^2\overline{Q}^2$, there are three 0^+ and three 2^+ $Q^2\overline{Q}^2$ around the $\rho\rho$ threshold which contribute

to $\gamma\gamma \to \rho\rho$. For 0^+ or 2^+ $Q^2\overline{Q}^2$ states, there are two isoscalars and one isotensor $Q^2\overline{Q}^2$. In the picture of $Q^2\overline{Q}^2$, there is a constructive interference between the isoscalar and isotensor amplitudes in the reaction $\gamma\gamma \to \rho^0\rho^0$. Consequently, a large cross section for $\gamma\gamma \to \rho^0\rho^0$ is obtained. For the reaction $\gamma\gamma \to \rho^+\rho^-$, such interference is destructive; thus, the cross section for $\gamma\gamma \to \rho^+\rho^-$ is smaller in comparison to $\gamma\gamma \to \rho^0\rho^0$. As a matter of fact, it is easy to obtain a 100 nb cross section for $\gamma\gamma \to \rho^0\rho^0$ at peak without any new parameter in the picture of $Q^2\overline{Q}^2$ states.

On the other hand, the TASSO Collaboration has found that for the reaction $\gamma\gamma \to \rho^0\rho^0$, 0^+ is dominant as $W_{\gamma\gamma} < 1.8$ GeV, and 2^+ is dominant as $W_{\gamma\gamma} > 1.8$ GeV. This result is consistent with the measurement of TPC/2γ. These results are consistent with the $Q^2\overline{Q}^2$ mechanism (Fig. 3).

$\underline{\gamma\gamma \to \rho^0\omega}$. In the same sense, the cross section of $\gamma\gamma \to \rho^0\omega$ can be explained by the $Q^2\overline{Q}^2$ model (Fig. 4).[7]

$\underline{\gamma\gamma \to K^*\overline{K}^*, \rho^0\phi, \omega\phi}$. Observation[8] of the reaction $\gamma\gamma \to K^{*+}K^{*-}$ in the 1.7–2.7 GeV region with a peak value of about 50 nb at about 1.9 GeV has been reported. The structure in the channel $K^{*0}\overline{K}^{*0}$ is observed[9] to be smaller than the $K^{*+}K^{*-}$ channel by a factor of $7.8 \pm 3.1 \pm 2.0$. The ARGUS mean upper limit[9] on the $\gamma\gamma \to \rho^0\phi$ cross section is 1.0 nb in the range of $W_{\gamma\gamma}$ between 1.8 and 2.2 GeV. The corresponding upper limit from TPC/2γ (Ref. 10) is about 6 nb in the $W_{\gamma\gamma}$ range of 2–2.5 GeV. The upper limit of the $\gamma\gamma \to \omega\phi$ cross section given by ARGUS[11] is 1.7 nb in the range of $W_{\gamma\gamma}$ between 1.9 and 2.5 GeV.

In the picture of $Q^2\overline{Q}^2$ states, there are two isoscalars and two isovectors which contribute to $\gamma\gamma \to K^*\overline{K}^*$. Among these four $Q^2\overline{Q}^2$, the two isovectors $Q^2\overline{Q}^2$ contribute to $\gamma\gamma \to \rho^0\phi$ and the two isoscalars contribute to $\gamma\gamma \to \omega\phi$. Without introducing the mixings between the two $Q^2\overline{Q}^2$ states with the same isospin, the $Q^2\overline{Q}^2$ picture[5,6] predicted very small cross sections for both $K^{*+}K^{*-}$ and $K^{*0}\overline{K}^{*0}$ channels and very large cross sections for $\gamma\gamma \to \rho^0\phi$.[6] On the other hand, there have been other theoretical attempts[12,13] to predict the $K^*\overline{K}^*$ productions in $\gamma\gamma$ collisions, but they are all confronted with difficulties in explaining the data.

In our recent paper,[14] it is pointed out that the predicted small $K^*\overline{K^*}$ cross sections in the picture of $Q^2\overline{Q}^2$ are due to the destructive interferences between two isoscalar states and also two isovector states. Since, in the MIT bag model calculation, all the 2^+ $Q^2\overline{Q}^2$ which decay to $K^*\overline{K^*}, \rho^0\phi$, and $\omega\phi$ dominantly essentially degenerate at 1.95 GeV, the slightest perturbation will cause them to mix pairwise in the channels. We introduce the mixing mechanism to explore its consequences.

After introducing the mixings, constructive interference is found for $\gamma\gamma \to K^{*+}K^{*-}$ betwen the isoscalar and isovector amplitudes, and this interference yields a large cross section for $\gamma\gamma \to K^{*+}K^{*-}$ around 1.9 GeV. Whereas destructive interference between these two amplitudes is found for the reaction $\gamma\gamma \to K^{*0}\overline{K}^{*0}$, this interference suppresses the cross section of $\gamma\gamma \to K^{*0}\overline{K}^{*0}$. The charged-to-neutral $K^*\overline{K^*}$ ratio is predicted to be about 4, which is compatible with the experimental measurement (Figs. 5, 6). By using the same mechanism, the amplitude of $\gamma\gamma \to \rho^0\phi$ is diminished. Consequently, the calculated cross section of this reaction is smaller than the original calculation by one order-of-magnitude. The mean value of the cross section in the range of $W_{\gamma\gamma}$ between 1.8 GeV to 2.2 GeV is 1.45 nb, which is compatible with the upper limits set by ARGUS and TPC/2γ. As in the earlier calculation, we still obtain a small cross section for $\gamma\gamma \to \omega\phi$. The mean value of the cross section in the range of $W_{\gamma\gamma}$ between 1.9 GeV and 2.5 GeV is about 0.34 nb, which is below the upper limit set by ARGUS.

3. $\underline{J/\psi \to \gamma + VV'}$. It is analogous to the VDM that a gluon can couple to a color octet vector quark pair; thus, we expect these $Q^2\overline{Q}^2$ states having larger $\underline{V} \cdot \underline{V}$ components can be produced in two hard gluon channels easily. Under this picture, these $Q^2\overline{Q}^2$ states can be produced in J/ψ radiative decays in the processes $J/\psi \to \gamma + VV'$ via the mechanism shown in Fig. 7. By using this mechanism, we compute the decay rates of $J/\psi \to \gamma\rho\rho$, $\gamma\omega\omega$, $\gamma K^*\overline{K^*}$, and $\gamma\phi\phi$.[15]

$$
\begin{aligned}
B\left(J/\psi \to \gamma(Q^2\overline{Q}^2)_{2^+} \to \gamma\rho\rho\right) &= 3 \times (0.8\text{–}1.4) \times 10^{-4} \\
B\left(J/\psi \to \gamma(Q^2\overline{Q}^2)_{2^+} \to \gamma\omega\omega\right) &= (0.8\text{–}1.4) \times 10^{-4} \\
B\left(J/\psi \to \gamma(Q^2\overline{Q}^2)_{2^+} \to \gamma\phi\phi\right) &= 0.7 \times 10^{-6} \\
B\left(J/\psi \to \gamma(Q^2\overline{Q}^2)_{2^+} \to \gamma K^*\overline{K^*}\right) &= (2.3\text{–}3.0) \times 10^{-5}
\end{aligned}
$$

4. Conclusions. The $Q^2\overline{Q}^2$ picture describes the reactions $\gamma\gamma \to VV'$ very well. In order to verify the existence of these $Q^2\overline{Q}^2$ states, it is important to search for them via a two-gluon channel; J/ψ radiative decays provide good opportunities for that. Due to the smallness of the decay rate of $J/\psi \to \gamma(Q^2\overline{Q}^2)_{2^+} \to \gamma VV'$, an e^+e^- collider with very high luminosity will be of significant assistance.

ACKNOWLEDGMENT

I would like to thank the Theory Group of SLAC for their hospitality.

REFERENCES

1. R. L. Jaffe, *Phys. Rev.* **D15** (1977) 281.
2. B. A. Li and K. F. Liu, *Phys. Rev.* **D28** (1983) 1636.
3. TASSO Collaboration, R. Brandelik *et al., Phys. Lett.* **97B** (1980) 448;
   TASSO Collaboration, M. Althoff *et al., Z. Phys.* **C16** (1982) 13;
   Mark II Collaboration, D. L. Burke *et al., Phys. Lett.* **103B** (1981) 153;
   CELLO Collaboration, H. J. Behrend *et al., Z. Phys.* **C21** (1984) 205;
   PLUTO Collaboration, Ch. Berger *et al., Z. Phys.* **C38** (1988) 521;
   TPC/2γ Collaboration, H. Aihara *et al., Phys. Rev.* **D37** (1988) 28.
4. JADE Collaboration, presented by H. Kolanoski, *Proc. of the 5th Int. Workshop on $\gamma\gamma$ Interaction,* Aachen (1983);
   CELLO Collaboration, H. J. Behrend *et al.,* DESY 88–185.
5. B. A. Li and K. F. Liu, *Phys. Lett.* **118B** (1982) 435, and *Erratum,* **124B** (1982) 550; *Phys. Rev. Lett.* **51** (1983) 1510; *Phys. Rev.* **D30** (1984) 613.
6. N. N. Achasov, S. A. Devyanin, and G. N. Shestakov, *Phys. Lett.* **108B** (1982) 134; *Z. Phys.* **C16** (1982) 55; *Z. Phys.* **C27** (1985) 99.
7. M. T. Ronan, LBL–26415 (December 1988).
8. ARGUS Collaboration, DESY 88–084 (June 1988).
9. ARGUS Collaboration, H. Albrecht *et al., Phys. Lett.* **198B** (1987) 255.
10. TPC/2γ Collaboration, H. Aihara *et al., Phys. Rev.* **D37** (1988) 28.
11. ARGUS Collaboration, H. Albrecht *et al., Phys. Lett.* **210B** (1988) 273.
12. S. J. Brodsky, G. Kopp, and P. M. Zerwas, *Phys. Rev. Lett.* **58** (1987) 443.
13. N. Achasov, V. Karnakov, and G. Shestakov, Novosibirsk, TPH–No. 32 (1987) 159.
14. B. A. Li and K. F. Liu, University of Kentucky, UK/89–02.
15. B. A. Li, Q. X. Shen, H. Yu, and K. F. Liu, *Phys. Rev.* **D32** (1985) 308.

FIGURE CAPTIONS

1. Diagram for the reaction $\gamma\gamma \to VV'$ with $Q^2\overline{Q}^2$ states as the intermediate states.
2. Diagram for the reaction $gg \to VV'$ with $Q^2\overline{Q}^2$ states as the intermediate states.
3. The calculated $Q^2\overline{Q}^2$ contributions to the $\gamma\gamma \to \rho^0\rho^0$ cross section (solid curve) and the $\gamma\gamma \to \rho^+\rho^-$ cross section (dashed curve) in comparison with the experimental data.
4. Cross section of $\gamma\gamma \to \omega\pi^+\pi^-$. The fitted curve was obtained from a four-quark model prescription.
5. Cross section for $\gamma\gamma \to K^{*+}K^{*-}$.
6. Cross sections for $\gamma\gamma \to K^{*0}\overline{K}^{*0}$ and $\rho^0\phi$.
7. Diagram for $J/\psi \to \gamma VV'$ with $Q^2\overline{Q}^2$ states as the intermediate states.

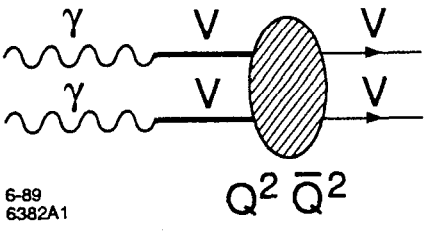

Fig. 1

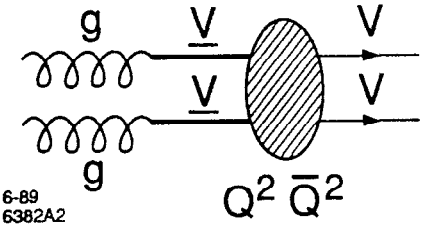

Fig. 2

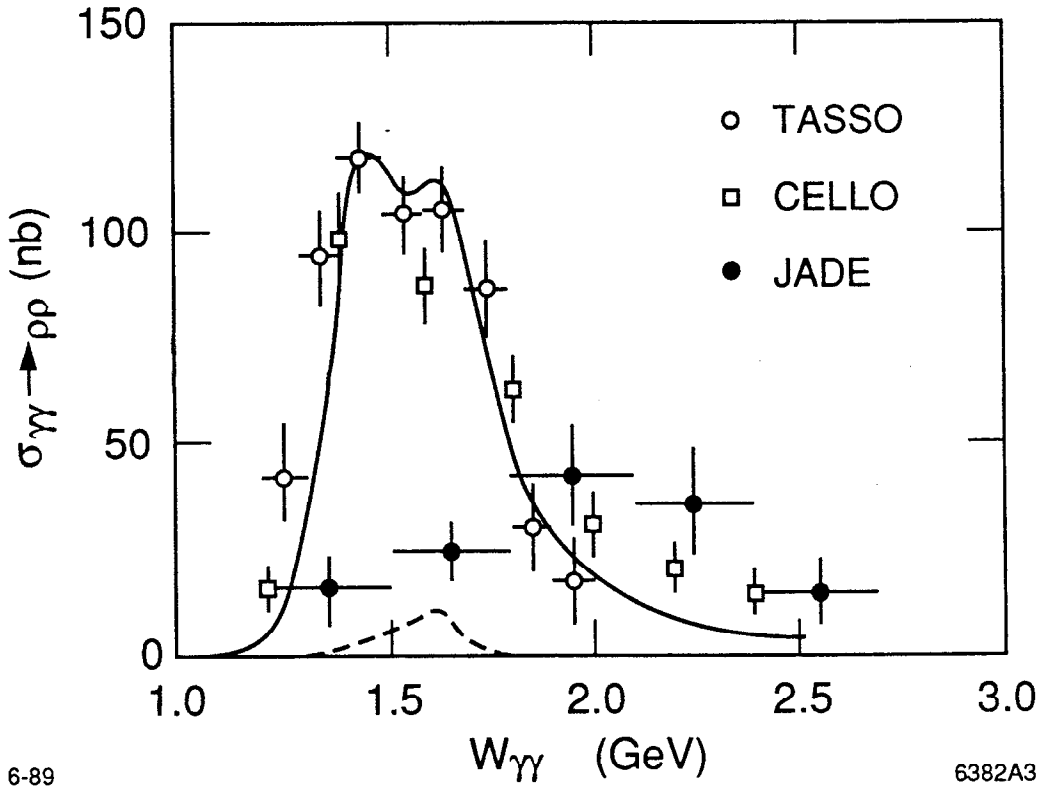
150
100
50
0
1.0
1.5
2.0
2.5
3.0
TASSO
CELLO
JADE
$\sigma_{\gamma\gamma \to \rho\rho}$ (nb)
$W_{\gamma\gamma}$ (GeV)
6-89
6382A3

Fig. 3

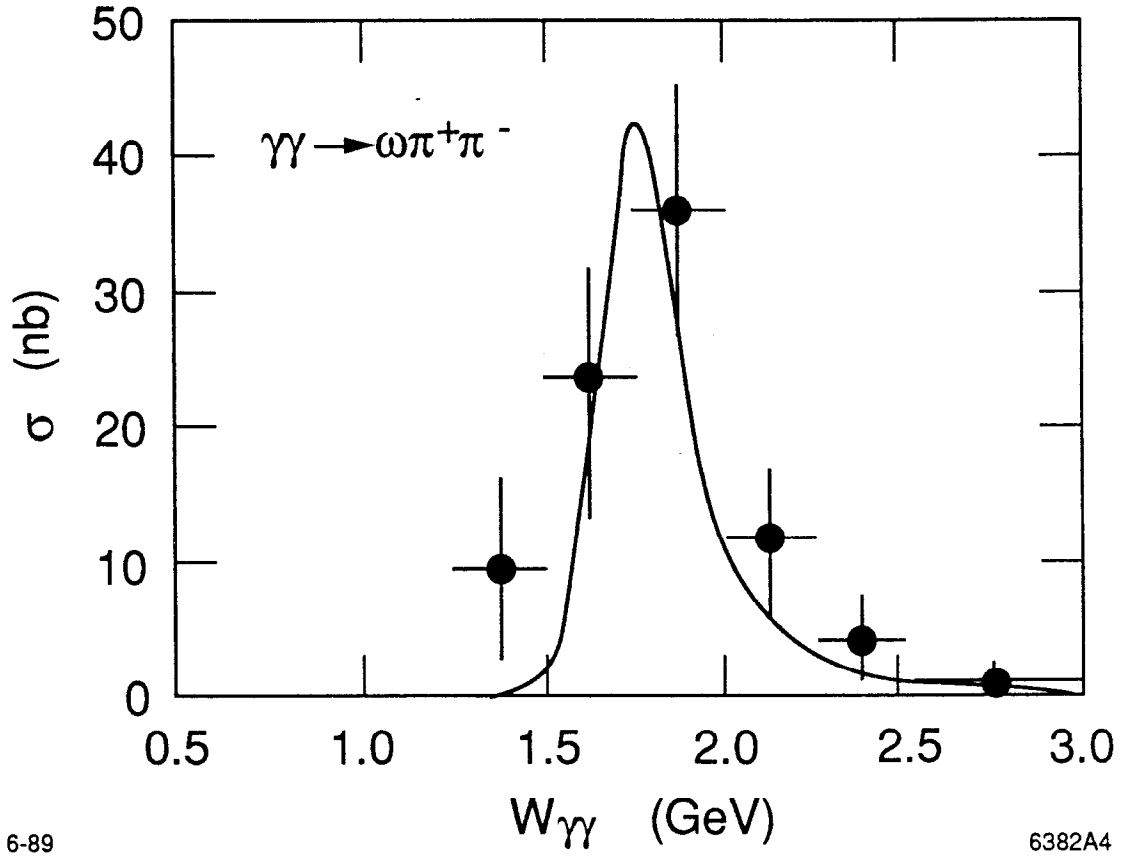

Fig. 4

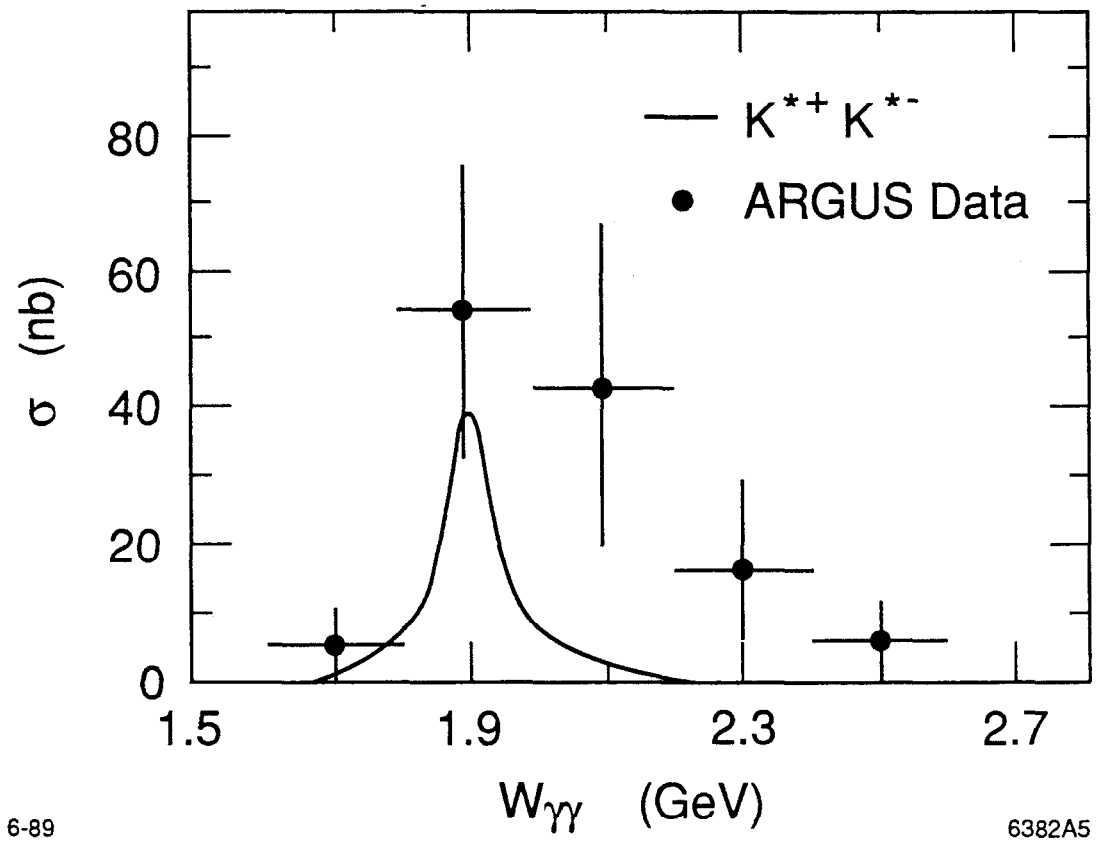
80
60
40
20
0
σ (nb)
1.5
1.9
2.3
2.7
$W_{\gamma\gamma}$ (GeV)
$K^{*+}K^{*-}$
ARGUS Data
6-89
6382A5

Fig. 5

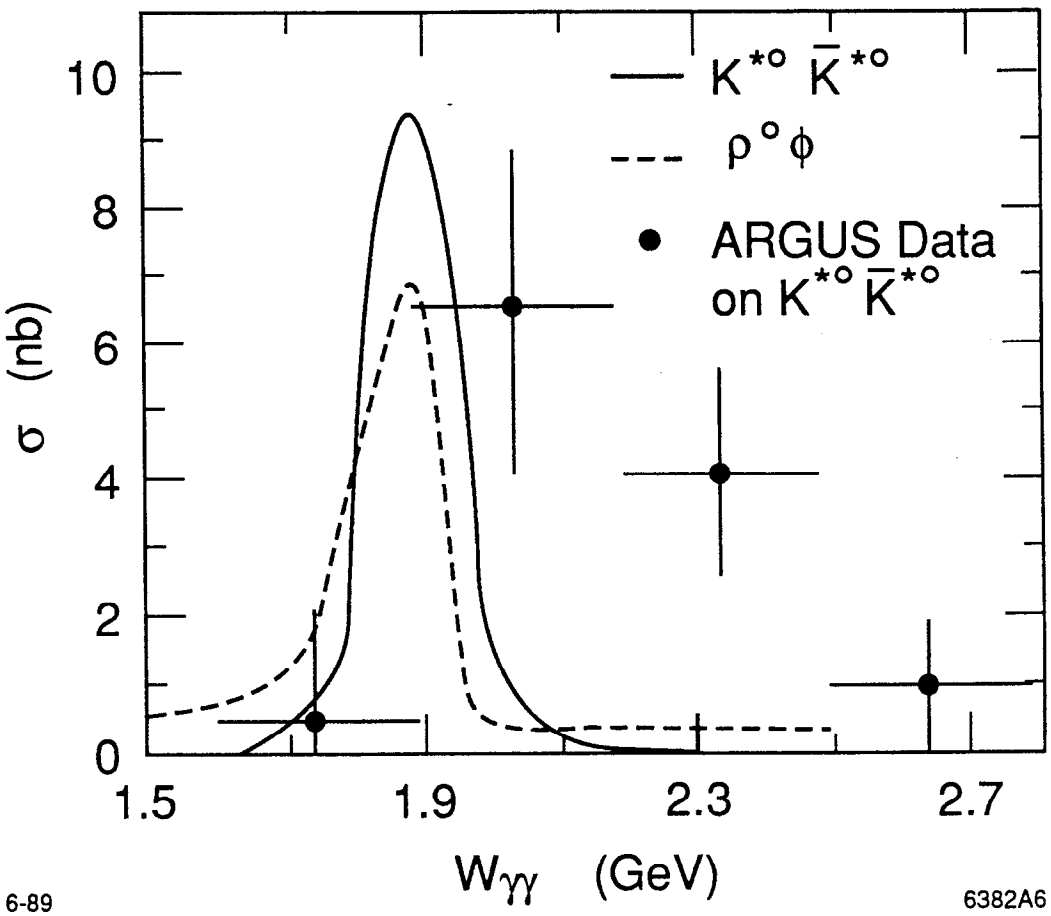
10
8
6
4
2
0
σ (nb)
1.5
1.9
2.3
2.7
$W_{\gamma\gamma}$ (GeV)
$K^{*0}\ \bar{K}^{*0}$
$\rho^0\phi$
ARGUS Data
on $K^{*0}\ \bar{K}^{*0}$
6-89
6382A6

Fig. 6

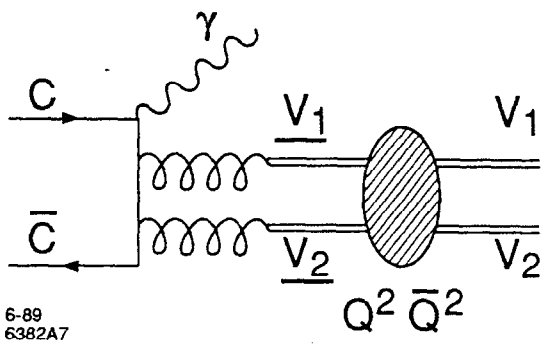

Fig. 7